# Wave-function mixture and composition for hybridized Zeeman states of P in Si

Shue-Chu Shen and Jing-Bing Zhu
*National Laboratory for Infrared Physics, Shanghai Institute of Technical Physics, Academia Sinica, Shanghai 200083, People's Republic of China*

Yao-Ming Mu
*Chinese Center of Advanced Science and Technology (World Laboratory), P.O. Box 8730, Bejing 100080, People's Republic of China and National Laboratory for Infrared Physics, Shanghai Institute of Technical Physics, Academia Sinica, Shanghai 200083, People's Republic of China*

Pu-Lin Liu
*National Laboratory for Infrared Physics, Shanghai Institute of Technical Physics, Academia Sinica, Shanghai 200083, People's Republic of China*
(Received 30 July 1993)

We report the experimental determination of the wave-function mixture and composition for hybridized Zeeman states of P in Si and give a related theoretical discussion. The intensity evolution of the Zeeman transitions near the anticrossing region for the isolated P donors in highly pure Si has been measured quantitatively by means of high-sensitivity and high-resolution photothermal ionization spectroscopy. The wave-function compositions and their evolutions with magnetic field for the hybridized Zeeman states of bounded electrons of impurities have been deduced from the measurement. A variational calculation in the framework of the effective-mass approach has been performed to estimate theoretically the wave-function compositions, and a comparison has been made between the theoretical results and experimental ones.

## I. INTRODUCTION

The hybridization between microscopic states, which interact strongly with each other in condensed matter, is a general phenomenon of interest, and has long attracted attention.[1-3] Taking electronic states in semiconductors, for example, there is hybridization and mixture between $d$ states of magnetic ions and $p$ states of anions in semimagnetic semiconductors,[3-5] those between heavy and light holes as well as between conduction band electrons of $\Gamma$ and $X$ states in quantum well structures,[6-8] those between Zeeman levels with the same parity and different main quantum numbers of donors in the semiconductors Si and Ge,[9-12] and hybridization of electron states with phonons or other microscopic states.[3,13] When hybridization between two electronic states occurs, they repulse each other in energy, which lifts the degeneracy of the states. If the energies of two strongly interacting states change with certain parameters, such as the wave vectors, the width of the quantum well, the magnetic field intensity, and the configuration of the measurement, adjusting these parameters can change the energy relation between the two states. Thus the hybridization between states and its evolution can be investigated experimentally. Again taking the hybridization of Zeeman levels of donors in Si as an example, since the rates at which different Zeeman levels shift with magnetic field are different, the transitions with the same parity and different main quantum numbers, which should cross under certain magnetic fields due to the different shifts with magnetic field, repulse each other, or "anticross," if the experimental configuration is selected such that it makes the perturbative Hamiltonian term causing the hybridization and wave-function mixture nonzero. The energy displacement between two hybridized states caused or added by the repulsion is determined by the strength of interaction which is related with the original energy difference between the two states. Thus the hybridization and anticrossing between Zeeman levels with the same parity and different quantum numbers occurs in certain regions of energy and magnetic fields.

Many theoretical methods and models[1-6,9-12] have been developed up to now, to investigate and calculate the energy dispersion or its relation with the perturbation (magnetic field, well width of the quantum well, etc.) for various hybridized states. At the same time, many of the experimental investigations have also been made which have revealed the anticrossing between two hybridized levels and proved the theoretical expectation as well as the dispersion relation given by theoretical calculation.[3,4,9,13-17] However, there is to our knowledge no report up to now on experimental results for the wave-function composition and its evolution along with a wave vector or extra perturbation for the hybridized states, though it might be deduced from the measured energy relation of hybridized states. The wave function of hybridized states can be a linear combination of the original states, based on a comparison with the linear combination of atomic orbits used in the calculation of the energy band for bulk materials or quantum wells or based on consideration of perturbation theory. Thus the wave function of a hybridized state can generally be written as

 

$$\phi = \sum_i C_i \phi_i \ , \tag{1}$$

where the $C_i$ are the expansion coefficients. It has been mentioned that we have not seen any report on the experimental investigation for the direct demonstration of the wave-function composition of a hybridized states shown as Eq. (1), which is not surprising if one realizes the difficulty in such an investigation.

We report in this paper the direct experimental determination of the wave-function mixture and composition for the hybridized Zeeman states of a phosphorus donor in Si and a theoretical discussion of the results. For some of the "anticrossing points" caused by hybridization between Zeeman levels of P in Si, there are only two levels (states) which hybridize with each other, and, furthermore, their oscillator intensities for dipole transitions are quite different, which makes it possible to measure the systematic evolution of the intensities of Zeeman transitions in the anticrossing region of the magnetic field by means of the high-sensitivity and high-resolution photothermal ionization spectroscopy.[18–20] Thus, the expansion coefficients $C_i$ and their evolution, i.e., the wave-function compositions of hybridized Zeeman states and their change with the strength of interaction can be directly measured from the systematical evolution of transition intensities. A variational calculation in the framework of the effective-mass approach has been also made in this paper to theoretically estimate the wave function of the hybridized states and to compare it with the experimental results.

## II. EXPERIMENT

The samples used are highly pure silicon cut along the $\langle 111 \rangle$ direction and with a phosphorus concentration of $10^{12}$ cm$^{-3}$ as the main residual impurity. The reason for the selection of highly pure samples is to make sure that all donors in the samples can be treated as isolated centers and the overlapping of their wave functions can be neglected even though they are in excited states with not too high quantum numbers ($n=4$, for example). Furthermore, high purity is also important to avoid the nonintrinsic broadening of spectral lines of transitions so as to observe the evolution of the transition intensities without obscurity. The reason for cutting samples along the $\langle 111 \rangle$ direction is to make it easy to observe the anticrossing phenomenon between Zeeman levels since Hamiltonian terms, which cause the hybridization of the states, have maximal values while the magnetic field is oriented along the $\langle 111 \rangle$ crystal axis. Moreover, all ellipsoidal valleys of the conduction band of Si are equivalent to the orientation of the magnetic field so as to simplify the theoretical treatment and the comparison between theoretical and experimental results.

The Zeeman splits and shifts are measured by means of the photothermal ionization spectroscopy under the magnetic field. The integrated intensities of various Zeeman transitions and their evolution during the hybridization are recorded at a high ratio of signal to noise in the region of the magnetic field from 0 to 10 T. It should be mentioned that one cannot see any transition line for such highly pure samples by the use of a conventional infrared absorption measurement. The magnet used in this experiment is a superconducting magnet of Oxford with the highest magnetic field of 11 T at 4.2 K. The samples are mounted on the cold finger of the inner Dewar of the magnet and the infrared radiation coming from a Fourier transform spectrometer is transferred onto the sample via a light pipe system with a transmission efficiency of 40%. The configuration of the measurement is selected to be $\mathbf{B}||\mathbf{k}||\langle 111 \rangle$ axis—here $\mathbf{k}$ is the wave vector of incident infrared radiation—and thus the electrical field of the incident light is perpendicular to the static magnetic field. The temperature of the samples during the measurement is 15 K.

## III. EXPERIMENTAL RESULTS

Figure 1 shows the photothermal ionization spectroscopies of P in highly pure Si in the wave-number region of 300–350 cm$^{-1}$ and under different magnetic fields from 0 to 10 T with the configuration of $\mathbf{B}||\mathbf{k}||\langle 111 \rangle$. The abscissa of the figure is the wave number of incident light and the vertical coordinates are the responses of photothermal ionization $2P_{\pm}$, $3P_0$, $4P_0$, $3P_{\pm}$, etc., which shows the donor transitions from the ground state $1S(A_1)$ of phosphorus. There are altogether 33 spectra recorded under different magnetic fields and we show part of them in Fig. 1, where from the bottom to the top of the figure the spectra are recorded at every 0.5 T for

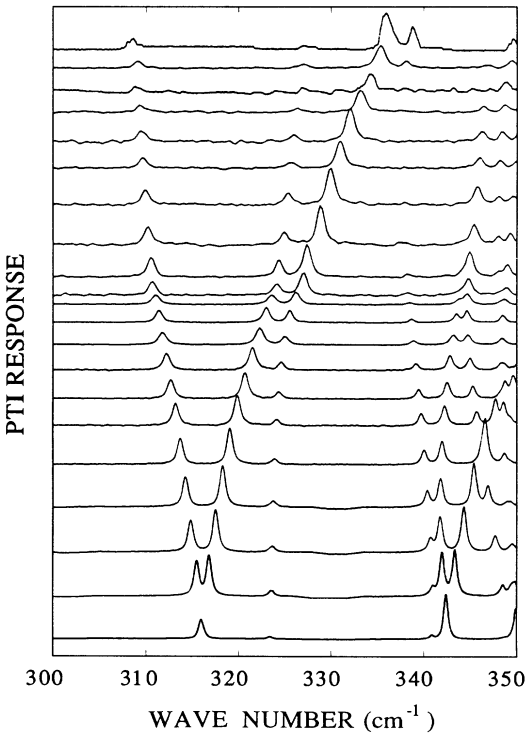


FIG. 1. Photothermal ionization spectroscopies of P in highly pure Si in the wave-number region of 300–350 cm$^{-1}$ and under different magnetic fields from 0 to 10 T with the configuration of $\mathbf{B}||\mathbf{K}||\langle 111 \rangle$.

the magnetic fields from 0 to 10 T. There are more spectral lines as well as their Zeeman splits and shifts above the wave number of 350 $cm^{-1}$. We will identify and discuss them elsewhere due to their complication. It is seen clearly from the figure that there is not any evidence of additional spectral lines between splitting transition lines $1S \rightarrow 2P_-$ and $1S \rightarrow 2P_+$, which indicates the high accuracy of the sample orientation. Thus one can neglect the experimental error related with orientation while the data are treated and discussed. The most attractive results shown in Fig. 1 are the repulsion with each other (anticrossing) for the transition lines of $1S \rightarrow 2P_+$ and $1S \rightarrow 3P_0$ as well as the systematic evolution of their intensity under the magnetic field around 5 T. Another anticrossing phenomenon occurs at $B \approx 10$ T and even more rapid intensity exchange is observed at this anticrossing. Here two hybridized states are original $3P_0$ and $4P_0$ under low magnetic fields ( $<4$ T). The highest magnetic field used in this measurement is 10 T and it can be expected from the figure that the transition intensities for the two spectral lines will evolve similarly to the anticrossing occurring at $B \approx 5$ T.

Figure 2 summarizes the experimental results of Zeeman splits and shifts as the functions of magnetic fields for several transition lines with lower quantum numbers of phosphorus donors in highly pure Si under the experimental configuration of $\mathbf{B}||\mathbf{k}||\langle 111\rangle$. These spectral lines can be identified as transitions from $1S(A_1)$ to $2P_-$, $2P_+$, $3P_0$, $4P_0$, $3P_-$, and $3P_+$, respectively, from the bottom to the top of the figure at a lower magnetic field ( $<1$ T, for example). It will be seen later that the identification of the transitions will no longer follow the above order; that is, some of them may change the characteristics of the transition at a higher magnetic field, though they have been assigned to the same processes in some literatures, whether at lower or higher fields. Figure 2 clearly illustrates the results implied in Fig. 1 that the transitions $1S \rightarrow 2P_+$ and $1S \rightarrow 3P_0$, which should be crossed with each other if there were no interaction between them, repulse each other due to the hybridization under magnetic fields around 5 T. The energy difference between them is $\Delta E \approx 4.1$ $cm^{-1}$ $\approx 0.5$ meV under this magnetic field. The two transitions that are assigned as $1S \rightarrow 3P_0$ and $1S \rightarrow 4P_0$ under lower fields also hybridize and repulse each other under a magnetic field of about 10 T with $\Delta E \approx 0.5$ meV. It can also be seen from Fig. 2 that there are also hybridization and repulsion between transitions $1S \rightarrow 4P_0$ and $1S \rightarrow 3P_-$ under magnetic fields of $B \approx 0.8$ T though the interaction is weaker and the minimum energy difference between them is only $\Delta \approx 1.5$ $cm^{-1}$, as the magnetic field when the hybridization occurs is also lower.

## IV. WAVE-FUNCTION MIXTURE AND COMPOSITION FOR HYBRIDIZED ZEEMAN STATES

Figure 3 summarizes the observed results of integrated intensities for three spectral lines of Zeeman transition, which are assigned as $2P_+$, $3P_0$, and $4P_0$ under a weak magnetic field as a function of the magnetic field for one sample. In comparison with Fig. 2, it can be seen that optical transition intensities of the spectral lines, which are identified as $1S \rightarrow 2P_+$ and $1S \rightarrow 3P_0$ under a weak magnetic field, evolve in opposite direction in the region of a magnetic field where $2P_+$ and $3P_0$ energy levels hybridize with each other; thus under a stronger magnetic field, for example, $B \approx 8$ T, the relation of their intensities is opposite to that under a weak magnetic field. A similar behavior can also be observed from transitions $1S \rightarrow 3P_0$ and $1S \rightarrow 4P_0$ ($3P_-$) identified under a weak magnetic field. In the region of $B = 6$–$9$ T, $1S \rightarrow 4P_0$ transition is so weak that it falls into the background noise and can no longer be observed. However, under $B > 9$ T its transition intensity greatly increases with a strong decrease in the transition intensity of $1S \rightarrow 3P_0$ hybridized with $1S \rightarrow 4P_0$. Therefore, from Fig. 3 it can be predicted that their transition intensities would be equal to each other, then would evolve in opposite direction as shown by the dashed line. The change of the transition intensity of $1S \rightarrow 4P_0$ in the region of magnetic field 0–4 T is very complicated, but it can be concluded from a detailed investigation of Figs. 1–3 that it is related to hybridization among $4P_0$, $3P_-$, and $3P_+$ or even $4P_-$.

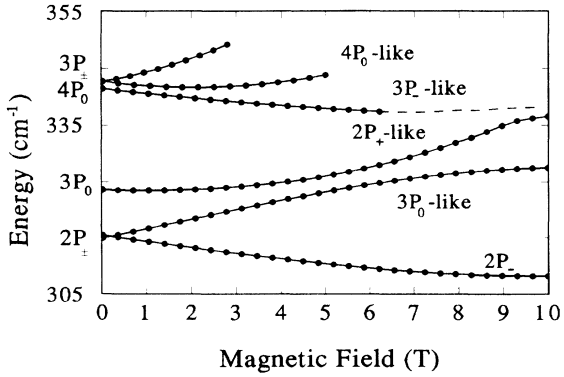


FIG. 2. The experimental results of Zeeman splits and shifts as the functions of magnetic fields for several transition lines with lower quantum numbers of phosphor donors in highly pure Si under the experimental configuration of $\mathbf{B}||\mathbf{K}||\langle 111\rangle$.

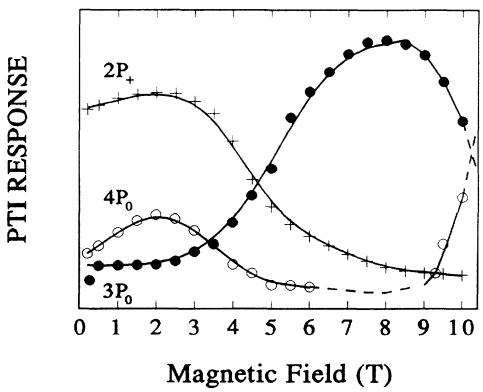


FIG. 3. Observed results of integrated intensities of three Zeeman transition spectra as functions of magnetic field under the experimental configuration of $\mathbf{B}||\mathbf{K}||\langle 111\rangle$.

The hybridized state model can explain the evolution of transition intensities of Zeeman spectral lines with magnetic fields shown in Fig. 3. On the other hand, one can say that the evolution of Zeeman transitions intensities shown in Fig. 3 gives direct evidence that electronic states can hybridize and their wave functions can be really mixed under certain conditions. In the following, we shall discuss in detail the hybridization of $2P_+$ and $3P_0$ states. Our experimental configuration is definitely $\mathbf{B}||\mathbf{k}||\langle 111\rangle$ and donor states related to six elliptical valleys of the conduction band for Si are equivalent for the orientation of the magnetic field. At the same times, Fig. 2 also shows that the energy differences between them and other transitions are large enough in the hybridized region. Hence, their hybridization can be described simply by a two-level interaction model. In the spirit of Eq. (1), wave functions of interacting up and down states can be written as

$$\begin{aligned}\phi_u &= A_u\phi_{3P_0}+B_u\phi_{2P_+}\ ,\\ \phi_l &= A_l\phi_{2P_+}+B_l\phi_{3P_0}\ ,\end{aligned} \tag{2}$$

where the subscript $u$ indicates the wave function and expansion coefficient related to the up energy level and $l$ indicates the wave function and expansion coefficient related to the down energy level. We assume that the difference of thermal ionization rates for different excited states of donor electron can be neglected in the narrow region of energy studied in this paper, thus the intensity of photothermal ionization spectra is determined by dipole absorption intensity. We also assume that matrix elements of optical transition $\langle 1S|H_{eR}|2P_+\rangle$ and $\langle 1S|H_{eR}|3P_0\rangle$ change very slowly with magnetic field, i.e., we neglect the change of the matrix elements with magnetic field. Thus the expansion coefficients $A_u$, $B_u$, $A_l$, and $B_l$ as functions of the magnetic field can be obtained uniquely by fitting Eq. (2) to the experimental results in Fig. 3 and are shown in Fig. 4. The similar results can be obtained for hybridization between two energy levels near $B=10$ T and stronger change can be predicted, that is, the evolutions of expansion coefficients in the region of the hybridization are much quicker. Thus Figs. 3 and 4 indicate that the wave functions of $2P_+$ and $3P_0$ are certainly mixed in their hybridized zone. At $B=4.75$ T, the up and down states consist of the original wave functions in equal percentage (50% to 50%), i.e., they have been hybridized completely. Figures 3 and 4 also give the regions of magnetic field and energy where the wave-function mixture occurs. For $2P_+$ and $3P_0$ states, the region of magnetic field is about $\Delta B=7$ T $-3$ T $=4$ T, and that of energy is about $\Delta E=7.2$ cm$^{-1}$ $=0.9$ meV, i.e., hybridization and wave-function mixture between the two states can be neglected while their energy difference is larger than about 0.9 meV. Hence, Figs. 3 and 4 clearly show that, although the two hybridized states repulse each other in energy position, their wave functions mix fully. Moreover, the expansion coefficients $A^2_{u,l}$ and $B^2_{u,l}$, which indicate wave-function composition of hybridized states, cross each other at $B\approx 4.75$ T, thus the physical characteristics related to transitions exchange with each other. The Zeeman transition $1S\rightarrow 2P_+$ assigned under a weak magnetic field evolves into a transition in which $3P_0$ plays an important role at $B>4.75$ T, and it completely becomes a $1S\rightarrow 3P_0$ transition at $B\geq 7$ T. The evolution of the $1S\rightarrow 3P_0$ transition is opposite, which becomes the $1S\rightarrow 2P_+$ transition at $B>4.75$ T and again changes its physical characteristics of optical transition due to another hybridization with a higher-energy level. Therefore, at 5 T $<B<10$ T, spectral lines observed in Fig. 2 can be assigned as the transitions from $1S(A_1)$ to $2P_-$, $3P_0$, $2P_+$, $3P_-$, and $4P_0$, respectively, from low- to high-energy levels.

Figures 2 and 3 also show that Zeeman level hybridization and a wave-function mixture of P in Si can only occur between energy states with the same parity but different main quantum numbers.

## V. THEORETICAL INTERPRETATION

In order to interpret the experimental results discussed in the above sections and estimate energy dispersion and intensity evolution of optical transitions related to hybridized states, we have extended Faulkner's effective mass theory[12,21] by taking into account the effects of a magnetic field on the shallow donor states. The Zeeman energy levels and their hybridization as functions of magnetic

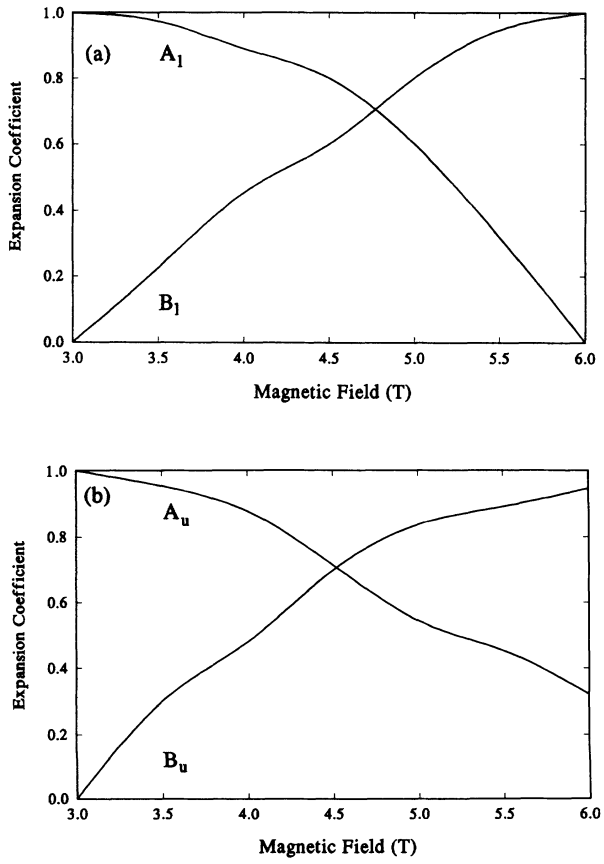


FIG. 4. Expansion coefficients of hybridized states at the region where $2P_+$ and $3P_0$ hybridize each other. (a) For down state and (b) for up state.

field are calculated by using the variational method.

Our variational wave functions $\varphi_{nlm}$ consist of normalized hydrogenic wave functions

$$\psi_{nlm}(x,y,z)=R_{nl}(\alpha_{lm},r)Y_{lm}(\theta,\varphi)$$

and take the following form:

$$\varphi_{nlm}=\left[\frac{\beta}{\gamma}\right]^{1/4}\psi_{nlm}\left[x,y,\left[\frac{\beta}{\gamma}\right]^{1/2}z\right], \tag{3}$$

$$R_{nl}(\alpha_{l,m},r)=\frac{2\alpha_{l,m}^{3/2}}{n^2}\left[\frac{(n-l-1)!}{[(n+l)!]^3}\right]^{1/2}\left[\frac{2\alpha_{l,m}r}{n}\right]^{l}\times\exp\left[-\frac{\alpha_{l,m}r}{n}\right]L_{n-l-1}^{2l+1}\left[\frac{2\alpha_{l,m}r}{n}\right], \tag{4}$$

where $\gamma=m_{\perp}/m_{\parallel}$, $\alpha_{lm}$, and $\beta$ are variational parameters. The number $N$ of orthonormal wave functions $\varphi_{nlm}$ is determined by the biggest principal quantum number $n_{\max}$ for the calculation. For example, if we consider the largest principal quantum number $n_{\max}=5$, $N$ is equal to 29 for even-parity states. The advantage of using hydrogenic variational wave functions is that the matrix elements of the effective-mass Hamiltonian including all magnetic-field terms can be expressed analytically.

The linear and quadratic magnetic field terms $H_1$ and $H_2$ in the Hamiltonian can be written as[12]

$$H_1=\gamma^*\left[\eta_{pm}L_xB_x+\eta_{pm}L_yB_y+L_zB_z+i\eta_{pm}(1-\beta)(yB_x-xB_y)\frac{\partial}{\partial z}\right], \tag{5}$$

$$H_2=(\gamma^*/2)^2[\eta_{pm}^2z^2(B_x^2+B_y^2)-2\eta_{pm}B_z(xB_x+yB_y)+(x^2+y^2)B_z^2+\gamma(yB_x-xB_y)^2], \tag{6}$$

where $\gamma^*=\hbar eB/2Rm_{\perp}C$, $R$ is Rydberg energy, and $\eta_{pm}=(\gamma/\beta)^{1/2}$. For the experimental configuration of $\mathbf{B}||\mathbf{k}||\langle 111\rangle$, the $H_1$ and $H_2$ can be written in the spherical coordinates as

$$H_{1a}=\frac{1}{\sqrt{3}}\gamma^*B[\eta_{pm}(L_x+L_y)+L_z], \tag{7}$$

$$H_{1b}=-\frac{i}{\sqrt{3}}\gamma^*B\eta_{pm}(\beta-1)\sin\theta(\cos\varphi-\sin\varphi)\times\left[r\cos\theta\frac{\partial}{\partial r}-\sin\theta\frac{\partial}{\partial\theta}\right], \tag{8}$$

$$H_{2a}=\frac{1}{3}\left[\frac{\gamma^*Br}{2}\right]^2[(1+\gamma)\sin^2\theta+\eta_{pm}^2\cos^2\theta], \tag{9}$$

$$H_{2b}=-\frac{1}{3}\eta_{pm}\left[\frac{\gamma^*Br}{2}\right]^2\sin(2\theta)(\sin\varphi+\cos\varphi), \tag{10}$$

$$H_{2c}=-\frac{1}{3}\gamma\left[\frac{\gamma^*Br}{2}\right]^2\sin^2\theta\sin^2(2\varphi). \tag{11}$$

In the present case, $H_{2a}$ is the main Hamiltonian term that causes the hybridization and mixture of Zeeman levels with same parity, different principal, and magnetic quantum number. The $H_{1b}$, $H_{2b}$, and $H_{2c}$ also contribute to the hybridization and mixture of these states and $H_{1b}$ plays an important role under low magnetic field.

The absorption coefficient $\sigma$ due to the shallow donor transition from the ground state $1S(A_1)$ to different excited states ex, for linearly polarized light of frequency $\omega$, takes the form

$$\sigma_{g-\mathrm{ex}}=\frac{4\pi^2e^2\omega}{nc}|\langle\phi_{\mathrm{ex}}|\mathbf{R}\cdot\mathbf{e}|\phi_g\rangle|^2\delta(E_{\mathrm{ex}}-E_g-\hbar\omega), \tag{12}$$

where $\mathbf{e}$ indicates the polarization direction of the incident light, $n$ is the refractive index of material, and $E_{\mathrm{ex}}-E_g$ is the energy difference between the excited and ground states. For unpolarized light, the electronic-dipole matrix element in the above equation is determined by

$$|\langle\phi_{\mathrm{ex}}|x|\phi_g\rangle|^2+|\langle\phi_{\mathrm{ex}}|y|\phi_g\rangle|^2+|\langle\phi_{\mathrm{ex}}|z|\phi_g\rangle|^2.$$

We have calculated these matrix elements as the functions of magnetic field using the wave functions and formulas in our previous paper.[12] Figure 5 shows our calculated results of absorption intensity for transitions from the $1S(A_1)$ state to excited states, which have been identified as $2P_+$, $3P_0$, and $4P_0$ states under a low magnetic field as functions of the magnetic field. It is seen from the figure that the wave-function mixture, the evolutions of transitional intensity, and the changes of the characteristics of transitions for $1S\rightarrow 2P_+$ and $3P_0$ spectral lines at $B\approx 5$ T due to hybridization between $2P_+$ and $3P_0$ Zeeman energy levels have been explained reasonably. However, our calculated results of the evolution of the wave-function mixture and state hybridization with the magnetic field are not in full agreement with the experimental measurement. Our predicted changes are much slower than that of experimental results. In fact, the wave-function mixture predicted by our theory is weaker than that of the experimental measurement and it happens in wider regions of magnetic field and energy.

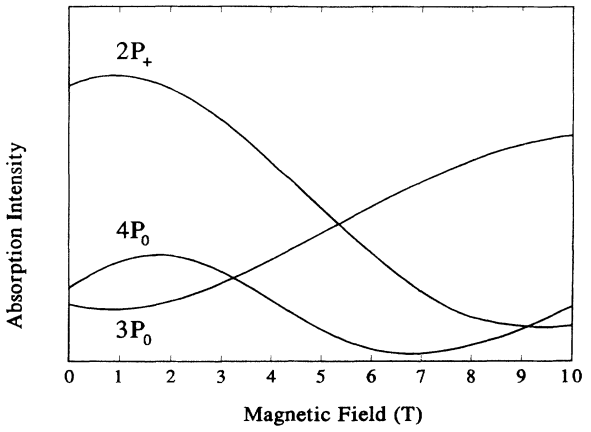


FIG. 5. Theoretically calculated results of the absorption coefficients for transitions from $1S$ to $2P_+$, $3P_0$, and $4P_0$.

Furthermore, our predicted magnetic field where anticrossing appears is a little higher than that of experimental results. At $B \approx 10$ T, for hybridization of transitions related to excited states, which are identified as $3P_0$ and $4P_0$ under a low magnetic field, the disagreement between theory and experiment is obvious. Although very strong changes of absorption intensity and characteristics of transitions for these spectra have been observed, one can only see some inkling from the theoretical curve of the $4P_0$-like transition. It must be noted that our predicted intensity evolution of $4P_0$ transition under low magnetic field is in good agreement with the experimental results. From the above discussion, it can be concluded that our theory and method can interpret energy level hybridization and wave-function mixture under lower magnetic field and obtain good agreement with experimental results. However, the disagreement between theory and experiment appears under a higher magnetic field and is enhanced with the increase of the magnetic field. It is not surprising that the effective-mass picture is an approximation and certain conditions must be met for its application, though we did not use perturbation approximation in taking into account the effect of magnetic field. In addition, the inconsistency may also owe, in part, to the variational wave functions that have consisted of hydrogenic wave functions at $B=0$. Therefore, a more satisfactory theory must be proposed to successfully interpret all experiment results related to the wave-function mixture and energy level hybridization.

## VI. CONCLUSION

Taking hybridization and the mixture of Zeeman levels of the P donor in Si as an example, we report the experimental evidence for the wave-function mixture and the linear combination of two microscopic electronic states in a condensed solid while they are hybridized. For Zeeman levels of P in Si, the wave-function mixture is so complete that the physical characteristics of states related to optical transitions are changed when they are hybridized. Zeeman level hybridization and the wave-function mixture of P in Si can occur only when the magnetic field is not parallel to the $\langle 001 \rangle$ direction. The regions of magnetic field and energy where hybridization and mixture can be observed are very narrow. At $\Delta E \geq 0.9$ meV, the observed hybridization between $3P_0$ and $2P_+$ can be neglected. The hybridization and mixture should occur in narrower regions of magnetic field and energy with an increase of the magnetic field. Thus the changes of wave functions related to hybridization may be stronger and the evolutions of physical characteristics of transition may be quicker for the hybridization occurring under a higher magnetic field.

The variational calculations in the framework of the effective-mass approach can explain qualitatively and semiquantitatively the hybridization and wave-function mixture of Zeeman levels of the P donor in Si. Obviously, more investigations are required in order to obtain better agreement between theoretical and experimental results.

[1]M. Born and K. Huang, *Dynamic Theory of Crystal Lattice* (Oxford University Press, New York, 1984), p. 82; K. Huang, Proc. R. Soc. London Ser. A **208**, 352 (1951).

[2]S. S. Mitra and N. E. Massa, in *Handbook on Semiconductors,* edited by W. Paul (North-Holland, Amsterdam, 1980), Vol. 1, p. 81.

[3]S. C. Shen, *Optical Property of Semiconductor* (Scientific Press, China, 1992), pp. 126, 271, 278, 320, 553, and 608.

[4]W. Shan, S. C. Shen, and H. L. Zhou, Acta Phys. Sin. **35**, 1290 (1986).

[5]S. Jiang and S. C. Shen, Phys. Rev. B **40**, 8017 (1989).

[6]J. N. Schulman and Y. C. Change, Phys. Rev. B **31**, 2056 (1985).

[7]G. Bastard, Phys. Rev. B **25**, 7584 (1982); **24**, 5693 (1981).

[8]Bangfen Zhu and Kun Huang, Phys. Rev. B **36**, 8102 (1987).

[9]B. Pajot, F. Merlet, G. Taravalla, and Ph. Arcas, Can. J. Phys. **50**, 1106 (1972); **50**, 2108 (1972).

[10]S. Zwerdling, K. J. Button, and B. Lax, Phys. Rev. **118**, 975 (1960).

[11]S. C. Shen, in *Eighth International Conference on Fourier Transform Spectroscopy,* edited by E. H. Korte, H. M. Heise, and H. W. Siesler, SPIE Proc. Vol. 1575 (SPIE, Bellingham, WA, 1991), p. 161.

[12]Y. M. Mu, J. P. Peng, P. L. Liu, S. C. Shen, and J. P. Zhu, Phys. Rev. B **48**, 10 864 (1993).

[13]S. C. Shen and J. H. Zhu, Acta. Phys. Sin. **34**, 56 (1985).

[14]C. H. Henry and J. J. Hopfield, Phys. Rev. Lett. **15**, 964 (1965).

[15]G. Livescu and O. Brafman, Solid State Commun. **35**, 73 (1980).

[16]G. Abstreiter, R. Huber, G. Trankle, and B. Vinter, Solid State Commun. **47**, 651 (1983).

[17]G. Abstreiter, R. Trommer, M. Cardona, and A. Pinczuk, Solid State Commun. **30**, 703 (1979).

[18]Z. Y. Yu, Y. X. Huang, and S. C. Chen, Phys. Rev. B **39**, 6287 (1989); Appl. Phys. Lett. **55**, 2084 (1989).

[19]Z. Y. Yu, Y. X. Huang, J. B. Zhu, W. Lu, and S. C. Shen, Chin. Sci. Bull. **35**, 1076 (1990).

[20]S. C. Shen, Z. Y. Yu, and Y. X. Huang, Int. J. IR mm Waves **11**, 595 (1990).

[21]R. A. Faulkner, Phys. Rev. **184**, 713 (1969).